



Globulispora mitoportans n. g., n. sp., (Opisthosporidia: Microsporidia) a microsporidian parasite of daphnids with unusual spore organization and prominent mitosome-like vesicles

Jiří Vávra ^{a,b,*}, Miroslav Hyliš ^c, Ivan Fiala ^{a,b}, Jana Nebesářová ^{a,c}

^a Institute of Parasitology, Biology Centre, Czech Academy of Sciences, České Budějovice, Czech Republic

^b Department of Parasitology, Faculty of Science, University of South Bohemia, České Budějovice, Czech Republic

^c Laboratory of Electron Microscopy, Faculty of Science, Charles University in Prague, Czech Republic



ARTICLE INFO

Article history:

Received 10 November 2015

Revised 22 January 2016

Accepted 3 February 2016

Available online 4 February 2016

Keywords:

Microsporidia

Fungi

Daphnia

Parasite

Mitosome

Phylogeny

ABSTRACT

The microsporidian parasite *Globulispora mitoportans*, n. g., n. sp., infects the intestinal epithelium of two species of daphnids (Crustacea: Cladocera). Mature spores are thin-walled and possess a novel type of polaroplast with a conspicuous part consisting of globules that occupies a large part of the spore volume. Both developmental stages and the spores possess large, electron-lucent vesicles enveloped by a double membrane and filled with an internal web of filamentous material, corresponding structurally to microsporidian mitosomes. The SSU rRNA phylogeny places *Globulispora* into a specific “Enterocytoplasmodium-like” clade, part of a large “non-enterocytozoonidae” clade, grouping a heterogenous assemblage of microsporidia infecting almost exclusively insects and crustaceans.

© 2016 Elsevier Inc. All rights reserved.

1. Introduction

Microsporidia are obligate intracellular eukaryotic parasites of animals and some protists, characterized by possessing within their spores an evaginable tube (“polar filament”, “polar tube”, “invasion tube”, “injection tube”) through which the spore contents are injected into cells of their hosts during spore germination (Vávra and Lukeš, 2013). The origin of microsporidia is not fully understood, but recent data indicate that microsporidia are related to fungi, either as a sister group of the “lower fungi” clade Cryptomycota, (James et al., 2013), as clade within Cryptomycota itself (Keeling, 2014), or as members of the newly proposed superphylum Opisthosporidia, which unites Microsporidia, Cryptomycota and algal parasites Aphelinida, and represents a phylogenetic sister clade to the “true” fungi (Karpov et al., 2014). Microsporidia are ubiquitous organisms with more than 1500 species described in about 200 genera (Vávra and Lukeš, 2013; Becnel et al., 2014). Arthropods (Crustacea and Insecta) are their main hosts (Becnel and Andreadis, 2014; Stentiford and Dunn, 2014), but many microsporidia occur in other animal phyla, vertebrates included.

Humans are hosts of several vertebrate-specific microsporidian species, but occasionally can be infected by non-specific microsporidia infecting invertebrates or unknown hosts (Snowden, 2014).

Because microsporidia are among the most common single-cell animal parasites, their origin and basal phylogeny are particularly interesting from the evolutionary point of view, but neither are well known. It is only recently that understanding of the phylogeny has increased (Keeling, 2014; Vávra and Lukeš, 2013) and it has been suggested that microsporidia may have originated in an aqueous environment. Microsporidia of aquatic invertebrates (especially those filtering water, e.g. the daphniids) are, thus, a group that may provide clues to the origin of these unique organisms. A microsporidium recently reported infecting the gut epithelium of a species of water flea (Crustacea, Branchiopoda), is claimed to represent a basal organism in the microsporidia tree, closest to the common ancestor at the Cryptomycota Rozella-Microsporidia branching point. This organism possesses a large “mitochondrium-like structure with a double membrane”, an organelle that is atypical both in structure and biochemical functions to mitosomes of other microsporidia (Haag et al., 2014). Here, we report the isolation of another microsporidian parasite from the gut epithelium of two daphnid species, which differs from other microsporidia described from the same host-tissue. This isolate is unique in structure among the

* Corresponding author at: Department of Parasitology, Faculty of Science, University of South Bohemia, České Budějovice, Czech Republic.

E-mail address: vavrajir@natur.cuni.cz (J. Vávra).

microsporidia and represents a new genus. The large and structurally complex mitosome-like vesicles in the cells contribute to the understanding of microsporidian mitosome structural diversity.

2. Material and methods

2.1. Collection of specimens and microscopy

Infected daphnids, *Daphnia pulex* (Leydig, 1860), and *Simocephalus vetulus* (Müller, 1776), were collected in 2013 in a large, nearly permanent forest marsh, near Běleč, Central Bohemia region, Czech Republic ($50^{\circ}3'12.240''N$, $14^{\circ}1'4.221''E$). Although the infection was frequent in *D. pulex* (about 5% infected), only three infected *S. vetulus* were found. Infected hosts and the parasite were examined by routine methods of light microscopy (LM) (Vávra and Maddox, 1976; Becnel, 2012) including spore immobilization on agar, negative staining using Burri Bacteriology Ink and measurement of spores using QuickPHOTO MICRO 3.0 (Promicra). For electron microscopy (TEM) the standard techniques and instruments described in Refardt et al. (2008) were used. Observations requiring high-resolution were made using Jeol 2010 200 kV electron microscope equipped with Gatan camera Orius SC 1000. Five infected specimens of *D. pulex* and two of *S. vetulus* were examined by TEM.

2.2. DNA isolation, PCR, and SSU rDNA sequencing

DNA was isolated from a single infected *D. pulex* female according to a protocol of Andreidis et al. (2013) in which, however, host tissues and spores were homogenized together. Single specimen isolation was selected in order to avoid possible contamination by other microsporidia present in the habitat. The specimen was placed in 0.5 ml microvial tube with equal volumes of 0.5 mm/0.1 mm (1:1) glass beads (BioSpec Products), 150 µl STE buffer (Fluka, BioUltra, pH 7.8) and was shaken in a Mini-Beadbeater (Biospec Products) for 30 s at maximum speed. Part of the mixture containing spore debris and spores was controlled by light microscope to ascertain that a single microsporidian species was present, another part was immediately incubated at 95 °C for 5 min and centrifuged at 14,000 g for 5 min. Supernatant was removed and 3 µl were used for PCR. Primers 18f and 1492r (Weiss and Vossbrinck, 1999) were used to amplify the SSU rDNA. PCR reaction (95 °C for 2 min; 30 cycles of 94 °C for 1 min, 50 °C for 1 min., 72 °C for 2 min; and 72 °C for 10 min) was conducted in a total volume of 25 µl, containing 25 pmol of each respective primer and GoTaq® Green Master Mix (Promega), according to manufacturer instructions. PCR product was separated using 1% agarose gel electrophoresis, extracted from the gel, purified using the DNeasy Tissue Kit® (QIAGEN) and prepared for automated sequencing with primers 18f, 530r, 530f, 1047r, 1061f and 1492r (Weiss and Vossbrinck, 1999) and BigDye® Terminator v3.1 Cycle Sequencing Kit (Applied Biosystems) on an 3130XL Genetic Analyzer (Applied Biosystems). Three PCR products were read.

2.3. Alignments and phylogenetic analysis

Sequences were aligned using MAFFT v6.626b (Katoh et al., 2005) with the E-INS-i multiple alignment method and default parameters. Alignment was cross-checked using SEAVIEW v3.2 (Galtier et al., 1996). Alignment included our novel microsporidian sequence and available GenBank sequences of representative closely related microsporidia. *Vavraia culicis* was set as the outgroup. Phylogenetic trees were calculated from the sequence alignment using maximum likelihood (ML), Bayesian inference (BI) and maximum parsimony (MP). ML analysis was done in RAxML v7.0.3

(Stamatakis, 2006) with a GTR + Γ model. MP was calculated in PAUP* v4.0b10 (Swofford et al., 2001) with a heuristic search, random addition of taxa and Ts:Tv = 1:2. Bootstrap support was calculated from 500 replicates in ML and 1000 replicates in MP analysis. BI was done using MrBayes v3.0 (Ronquist and Huelsenbeck, 2003) with the GTR + Γ model of evolution. Initially, MrBayes was run to estimate posterior probabilities over 1 million generations via 2 independent runs of 4 simultaneous Markov Chain Monte Carlo (MCMC) algorithms with every 100th tree saved. Tracer v1.4.1 (Rambaut and Drummond, 2007) was used to determine the burn-in period. The burn-in period was set to 10%, i.e. 1000 initial trees.

2.4. Topology tests

TreeGraph v2.0.47-206 beta (Stöver and Müller, 2010) was used to generate alternate topologies for the topological tests. Designed topologies in Newick format were specified in the assumption block and the data with ML parameters (the same generated by RAxML program for ML analysis) were executed in PAUP* to generate likelihood scores for each constrained tree. Resulted per-site log likelihood scores were analyzed for significant differences in CONSEL v6.1 (Shimodaira and Hasegawa, 2001), using three likelihood-based tests: approximately unbiased (AU), Kishino-Hasegawa (KH), and Shimodaira-Hasegawa (SH).

3. Results

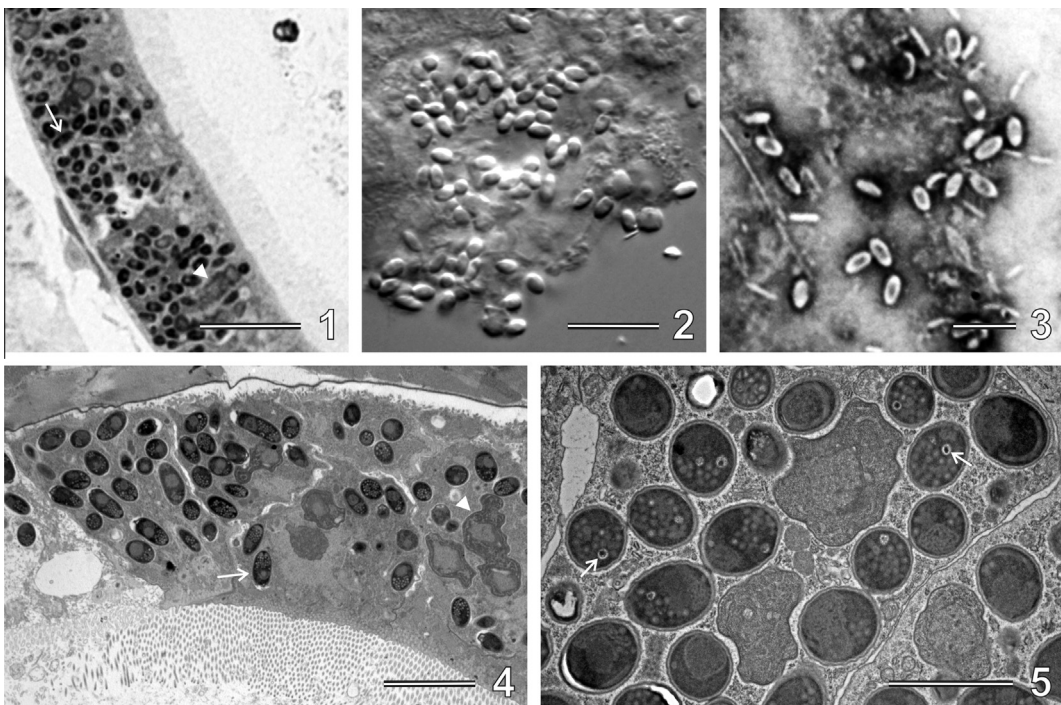
3.1. Light microscopy (LM)

The parasite infects the upper to middle part of the midgut epithelium of its hosts and the gastric ceca (Figs. 1 and 4). Diffuse infiltration of the epithelium by parasites was typical (Fig. 1). Infected cells contained masses of parasite spores, ovoid to oval in shape ($2.5 \times 1.6 \mu\text{m}$ fresh, $2.5 \times 1.5 \mu\text{m}$ dry, negatively stained smears, $n = 10$). Spores occurred singly, not grouped (Fig. 2) and their shape was well preserved in dry, negatively stained smears (a diagnostic character, see Fig. 3).

3.2. Electron microscopy (TEM)

Even at low power TEM allowed discrimination of the characteristic oval spores of the parasite interspersed with developmental stages (Figs. 4 and 5). At higher magnification, the developmental stages were shown either as small, irregularly lobed ribbon-like sporogonial plasmodia with several isolated nuclei or uninucleate cells originating by plasmotomy of plasmodia (Figs. 6–9). The cytoplasm contained a dense population of ribosomes, most of them free, some associated with endoplasmic reticulum cisternae (Fig. 6). The plasma membrane of developmental stages was covered with a 20 nm thick, fuzzy granular layer of medium density (Fig. 10), indicating that all developmental stages observed belonged to the sporogony sequence. No merogonial stages were observed. All developmental stages were in direct contact with host cell cytoplasm.

A conspicuous structure in the developmental stages was one or several large electron-lucent vesicles containing irregularly dispersed membranous material. These vesicles typically adhered to the nuclei (Figs. 8 and 9). Vesicles were variable in size (evidently due to the plane of section), measuring from $300 \times 80 \text{ nm}$ to $1500 \times 100 \text{ nm}$. These vesicles divided when the nucleus divided evidenced by a long extension connecting the respective divided nuclei (Fig. 7). At higher magnification the vesicles were observed to be enveloped by a double membrane and contained a loose web of filamentous material of medium density and sometimes clump



Figs. 1–5. LM and low power TEM views of infected tissues and spores of *Globulispora mitoportans*, n.g., n. sp. Fig. 1. Semithin section of a heavily infected midgut of *Daphnia pulex*. Toluidine blue staining. Developmental stage is at arrowhead, spores are at arrow. (Scale bar = 10 µm.) Fig. 2. Fresh spores in Nomarski contrast. (Scale bar = 10 µm.) Fig. 3. Spores on dry smear after negative staining by Burri-Bacteriology Ink. (Scale bar = 5 µm.) Fig. 4. Low power EM view of infected midgut of *D. pulex* showing the presence of developmental stages (arrowhead) and spores (arrow). The midgut integrity is maintained and spores and developmental stages are evenly distributed in the infected tissue. (Scale bar = 5 µm.) Fig. 5. The characteristic oval spores with thin walls and numerous lucent globules allow identification of the parasite at low power. Spore mitosomes (MLVs) are visible at low mag (arrows). (Scale bar = 2 µm.) (For interpretation of the references to color in this figure legend, the reader is referred to the web version of this article.)

of dense material (Figs. 11–13). In some vesicles the filamentous web material was arranged in a form somewhat resembling the inner membranes of mitochondria (Fig. 13). We call these vesicles “mitosome-like vesicles” (MLVs). We believe that they represent mitochondrial remnants, the mitosomes (see Section 5.2).

3.2.1. Mature spores

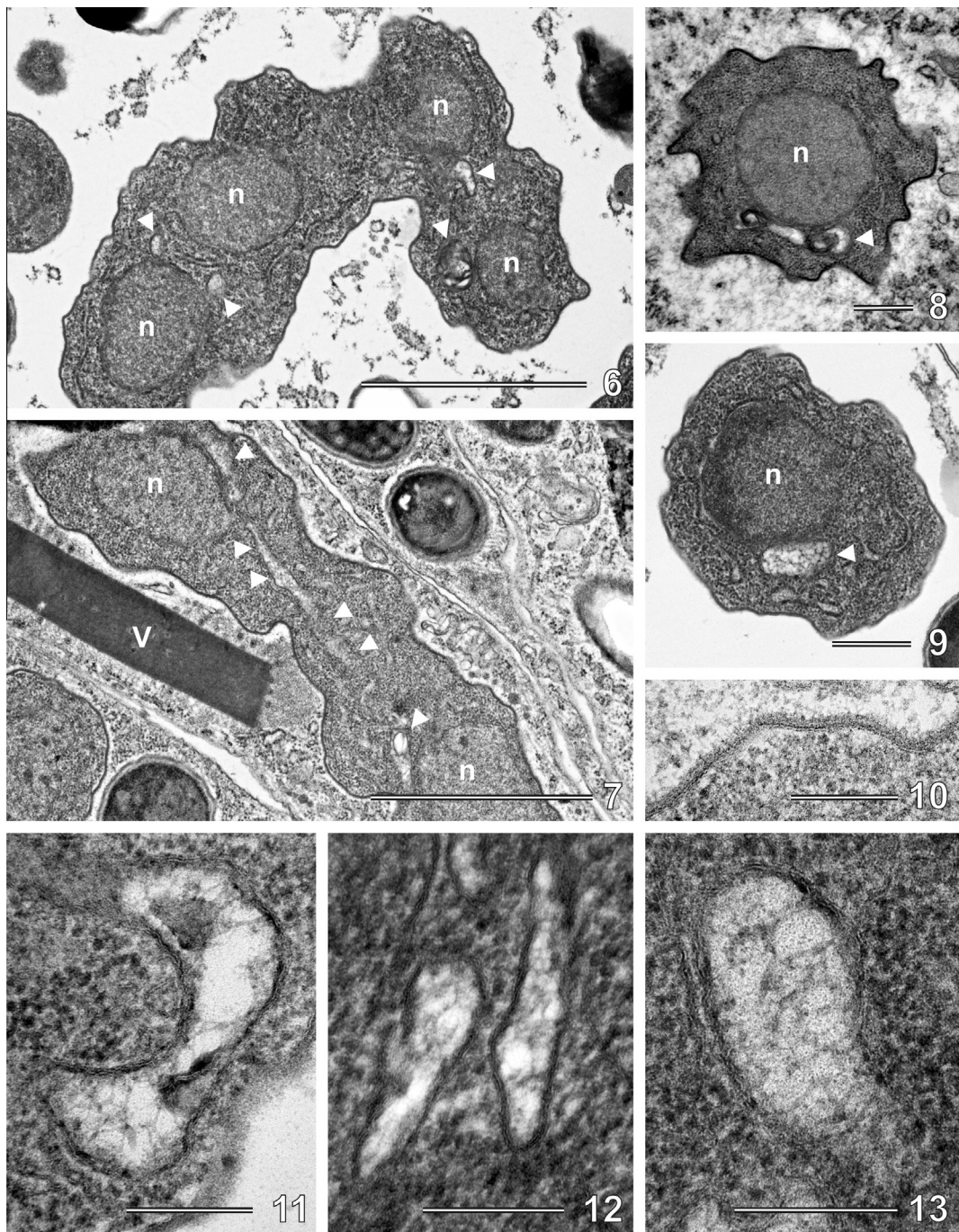
Low TEM magnifications showed three characters enabling immediate identification of spore identity; the absence of a thick, transparent chitinous wall typically present in typical microsporidia, the presence of small and numerous electron-lucent globules filling the anterior half of the spore, and the occurrence in the spore of one or a few relatively large transparent vesicles with a dense center (Figs. 5, 14 and 19). The description of these spore characters, of the spore polar filament and of a vacuolar area of “posterior vacuole” is presented in detail below.

3.2.1.1. The spore wall. The ovoid (Figs. 14 and 15) or elongate-ellipsoidal (Fig. 16) spores had thin walls, limited (from the spore interior outwards) by a plasma membrane and a single, 15–30 nm, finely granular layer of medium electron density (Figs. 14–17). This granular layer was evidently homologous to the endospore of classical microsporidia, but it is thin and less transparent. The rudimentary endospore was covered on the outside by a double layer of more dense material measuring 25–30 nm, representing the exospore (Fig. 17a and b). At the limit of resolution was a very fine membranous layer marking an outer covering of some spores (Fig. 17a and b). This outer layer formed a “sachet” around the spores when spores were released into a hypotonic fixative (Fig. 15). In addition, the spore is probably enveloped by a layer of poorly structured mucous-like material that emanates from

the exospore as noticed by the presence of a clear halo around the spores, interspersed with some fibrillar material at the limit of resolution (Fig. 14). A frequent structural marker of spores was a small nipple or ill-defined spore wall protrusion at the posterior end of spore where the posterior vacuole is formed in classical microsporidia (Figs. 14–16).

3.2.1.2. Spore contents: the polaroplast, spore mitosomes, polar filament, posterior vacuole. The spore contained a large, single nucleus, characteristically accompanied by a large formation (nearly the size of the nucleus) of a poorly resolved structure of medium electron density. This structure consisted of stacks of poorly preserved membranes with some ribosomes interposed between stacks and probably represents the rough endoplasmic reticulum (Figs. 16 and 18). The portion of the spore between the nucleus and spore anterior tip was filled with globules and membranes of the polaroplast; the remaining part of the spore was densely packed with ribosomes and contained three to five polar filament coils (Figs. 14 and 16). An ill-defined “empty” vacuolar space occurred at the posterior pole of the spore (Figs. 14–16). Some of these spore components differ markedly from those of classical microsporidia and deserve to be treated in detail.

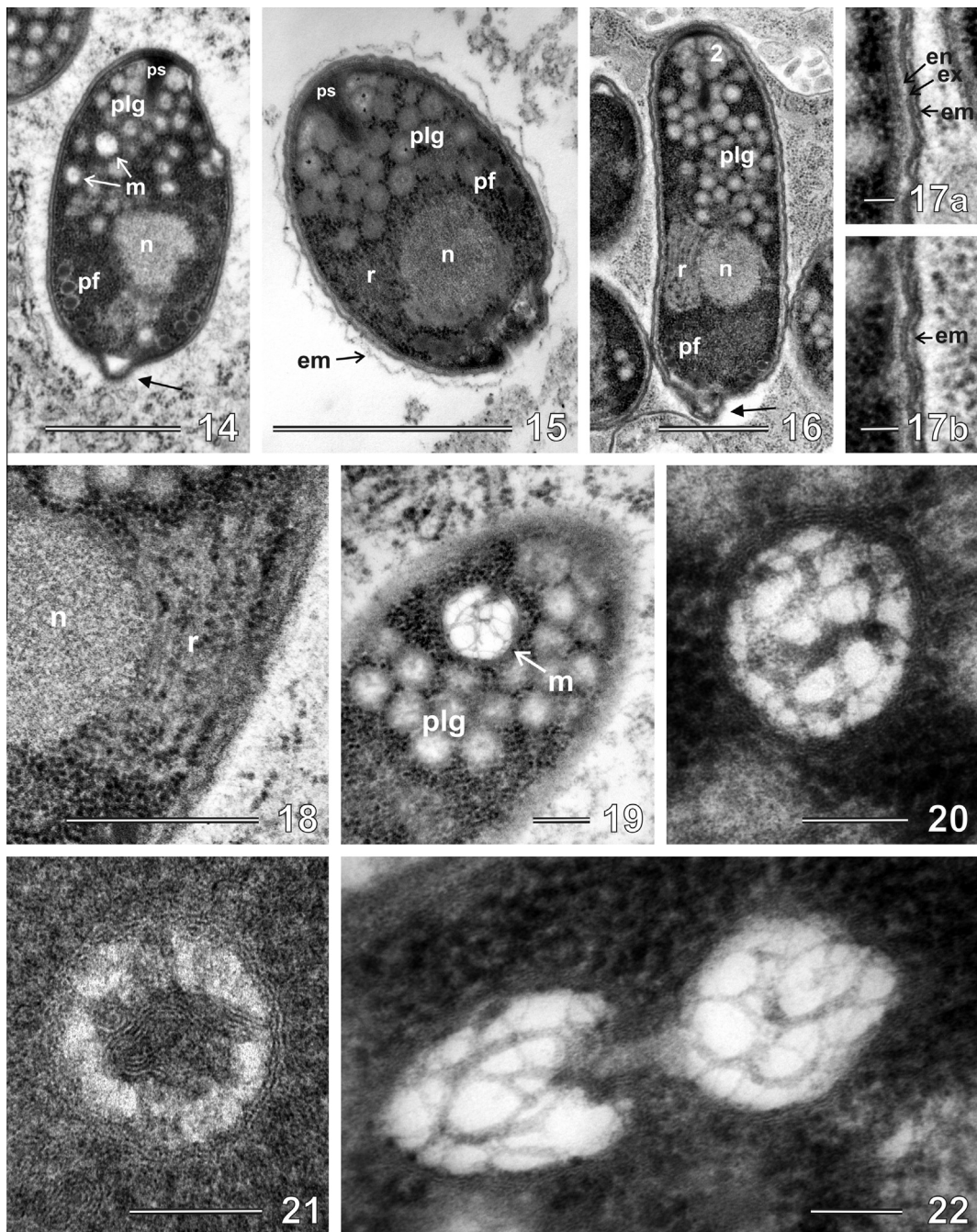
3.2.1.2.1. Polaroplast. Globules filling the anterior 1/3–1/2 of the spore (Figs. 5, 14–16 and 19) represented the most apparent part of the polaroplast. However, two less conspicuous parts complemented the polaroplast system. First, lamellar polaroplast occurred at the spore tip, and was represented by 5–8 closely adherent membranous lamellae (Figs. 23–25). These membranes were only rarely well preserved and occurred only in mature spores. The second part of the polaroplast was vacuolar, consisting of several inconspicuous vesicles of irregular outline situated just



Figs. 6–13. *Globulispora mitopartans*, n.g., n. sp. developmental stages and MLVs at higher power TEM. Fig. 6. Ribbon-like multinucleate plasmodium (nuclei = **n**; white arrowheads = MLVs). Scale bar = 2 µm. Fig. 7. Ribbon-like plasmodium after nuclear division (nuclei = **n**), showing the extended division path of a MLV (white arrowheads). Particle at **V** belongs to the cytoplasmic polyhedrosis virus which coexisted with *Globulispora* in the midgut of some *Daphnia* hosts. (Scale bar = 2 µm.) Figs. 8 and 9. Uninucleate presporal fragments of former plasmodia. Conspicuous MLVs (arrowheads) lie close to the nucleus (**n**) and show a reticulate internal structure. (Scale bar = 0.5 µm.) Fig. 10. External glycocalyx-like layer on the outerface of the plasma membrane of developmental stages. (Scale bar = 200 nm.) Figs. 11–13. Typical MLVs of *G. mitopartans*, n.g., n. sp. showing the MLV large size, its double membrane and irregular mesh of material in its interior. (Scale bar = 200 nm.)

below the polar sac and around the straight section of the polar filament (Figs. 23 and 25). The third part of the polaroplast was most conspicuous, represented the distinguishing character of the organism and consisted of individual round globules, 120–140 nm in size (Figs. 14–16, 19 and 25), limited by a single, difficult to distinguish membrane. Each globule was filled with finely granular material which gradually thickened toward the globule outer surface (Fig. 26). Cytoplasm with ribosomes separated individual globules (Figs. 23 and 25).

3.2.1.2.2. MLVs in spores. The anterior part of the spore contained one to several vesicles between the polaroplast elements described above. The vesicles were round in shape, around 230 nm in size, either seemingly empty or containing a ‘flimsy’ material at low magnification, or containing a clump of dense material in the center (Figs. 5, 14 and 19). Higher magnification showed that these vesicles were enveloped by a double membrane and contained filaments of medium electron density forming an irregular mesh (Fig. 20) or a dense clump of membranous material

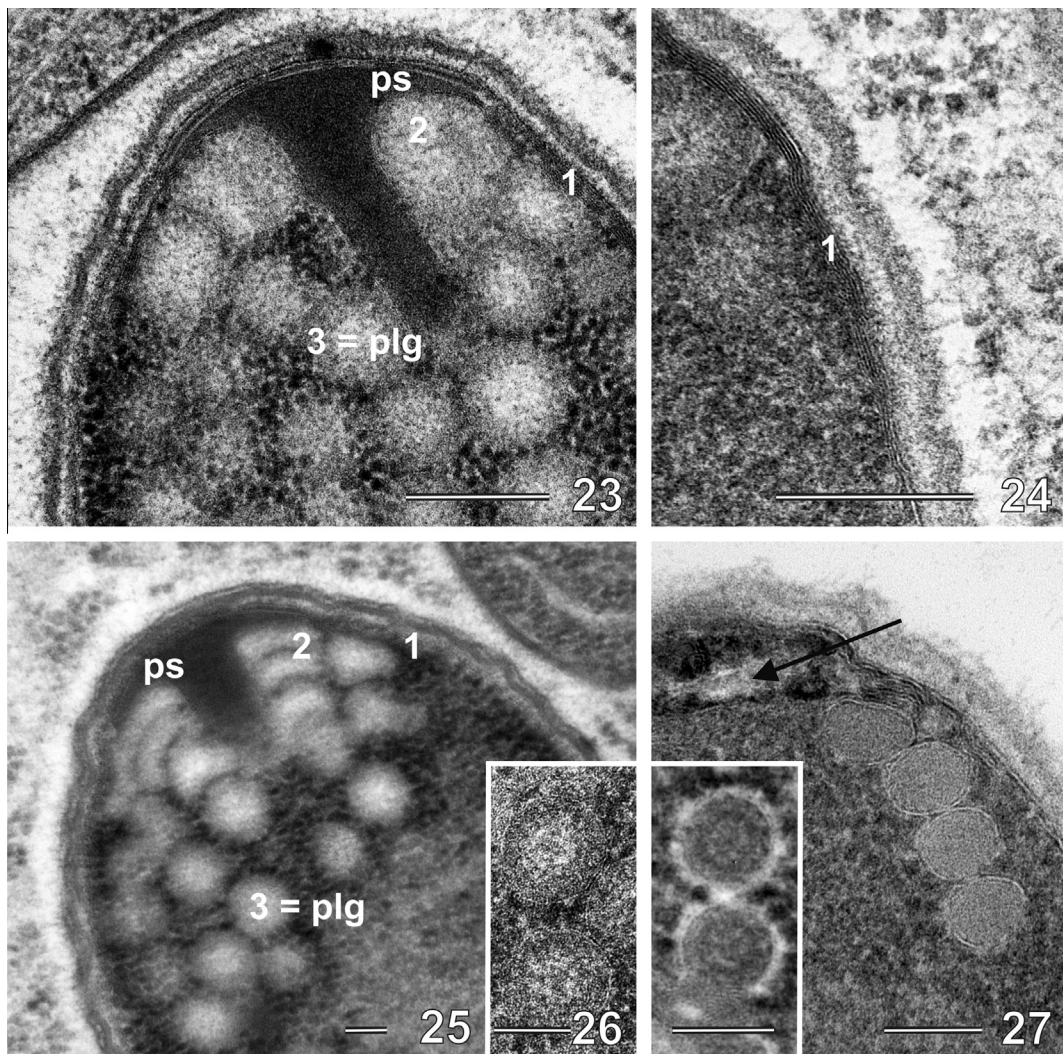


Figs. 14–22. Spores and sporal MLVs of *Globulipspora mitoportans*, n.g., n. sp. Figs. 14–18. Spore has a single nucleus (**n**), the anterior half of the spore contains the polar sac of the polar filament (**ps**), electronlucent globules (**plg**) and cisternae (**2**) of the polaroplast system. Note the characteristically nipple-shaped posterior pole of the spore (arrow). Coils of the polar filament are at (**pf**). Fig. 14 shows MLVs (white arrows, **m**). Fig. 15 shows a detached membranous layer of the exospore (**em**), shown also on Figs. 17a and 17b. Figs. 15 and 16 show at **r** the characteristic membranous area of the RER adjacent to the nucleus (see also Fig. 18). Figs. 17 a and 17b. The spore wall is thin, yet complex. The endospore layer is semitransparent and thin (arrow, **en**), and is bordered by a double layered exospore (arrow, **ex**). Another, membrane-like layer, usually tightly adherent to the exospore, borders the exospore (arrow, **em**). Fig. 18. Detailed view of the nucleus (**n**) with the characteristic adjacent membranous area of the RER (**r**). (Scale bars for Figs. 14–16 = 1 μm, for Figs. 17a and 17b = 100 nm, for Fig. 18 = 500 nm.) Figs. 19–22. MLVs in spores. Fig. 19. The MLV (white arrow, **m**) is situated in the anterior part of the spore, between the polaroplast globules (**plg**). (Scale bar = 200 nm.) Figs. 20–22. The MLV contains internal material, either in the form of a loose web (Figs. 20 and 22), or as a dense clump of membranes (Fig. 21). Fig. 22 shows division of the MLV. (Scale bars for Figs. 20–22 = 100 nm.)

(Fig. 21). Division of the vesicles was seen on occasion (Fig. 22). The double membrane configuration of these vesicles indicated that they are spore forms of the MLVs, evidently derived from the MLVs in developmental stages and acquiring their round form during sporogenesis.

3.2.1.2.3. Polar filament. Despite considerable modifications of the fixation procedure, we never achieved a satisfactory preservation of the filament with the complement of substructures known

from typical microsporidia. In our observations, the polar filament descended as an electron dense, structureless rod from the mushroom-like polar sac (Figs. 23 and 25), approached the spore wall and formed coils near the posterior pole of the spore. The filament had the same density as the polar sac, appearing as a continuation. No structure at the polar sac/polar filament interface known in typical microsporidia was seen in our material. Near the posterior pole of the spore, the filament formed 3–5 (but usually



Figs. 23–27. Polaroplast, polar filament and the posterior vacuole of *Globulispora mitoportans*, n.g., n. sp. spores. Figs. 23–26. The polar sac (**ps**) at the polar filament terminal, the lamellae of the first part of the polaroplast (**1**), a few cisternae of the second polaroplast component (**2**) and globules of the third part (**3 = plg**) are shown. Fig. 24. Detailed view of the polaroplast lamellae (**1**) from Fig. 23. Fig. 26. Detailed view of the globules of the third part of polaroplast from Fig. 23. (Scale bars for Figs. 23–25 = 200 nm; for Fig. 26 = 100 nm.) Fig. 27 and inset. Four coils of the polar filament. The filament shows trace of layering (inset with scale bar = 100 nm) Arrow shows the membrane limited space, corresponding to the posterior vacuole of canonical microsporidia. (Scale bar = 100 nm.)

4) isofilar, 70 nm thick coils, the most distal coil being somewhat thinner (Fig. 27). In some sections we observed trace of the layering inside the filament (Fig. 27-inset).

3.2.1.2.4. The posterior vacuole area. Many spores showed a small irregularity of the spore outline near the posterior pole of the spore (Figs. 14–16). A vacuolar area limited by a membrane occurred at this site representing what is known in typical microsporidia as the posterior vacuole (Fig. 27).

4. Phylogeny

The sequences of the three PCR products were identical. Phylogenetic analysis using maximum likelihood, Bayesian inference and maximum parsimony places the microsporidium on a separate branch within a clade containing the recently described *Enterocytoplasma artemiae* (infecting intestinal epithelium of *Artemia salina*; Rode et al., 2013), and four undescribed microsporidia from amphipod crustaceans with rRNA sequences deposited in GenBank (Fig. 28). Of these four microsporidia, three are parasites of gammarids from the Lake Baikal, the fourth isolate infects unidentified tissues of the invasive amphipod *Crangonyx* (Slohouber Galbreath

et al., 2010). The clade containing the *D. pulex* species in question was stable in all phylogeny analyses performed and formed one of the branches of a large clade containing a heterogenous assemblage of microsporidia infecting arthropods. The clade containing the *D. pulex* species was supported with high posterior probability in Bayesian inference (0.99), moderate bootstrap support in maximum parsimony (77%) and low bootstrap support in maximum likelihood (>50%). Bremer index was relatively high (8). Topology tests rejected all the alternative topologies with artificially assembled paraphyletic branching of the species of the studied clade containing the *D. pulex* species treated here (Supplementary Fig. S1). Due to stability in phylogeny analyses, the *D. pulex* species containing clade is proposed as the “*Enterocytoplasma-like*” clade (see Section 5).

5. Discussion

5.1. Host specificity

No differences were found between the parasites isolated from the two respective daphnid hosts. Unless future data will indicate

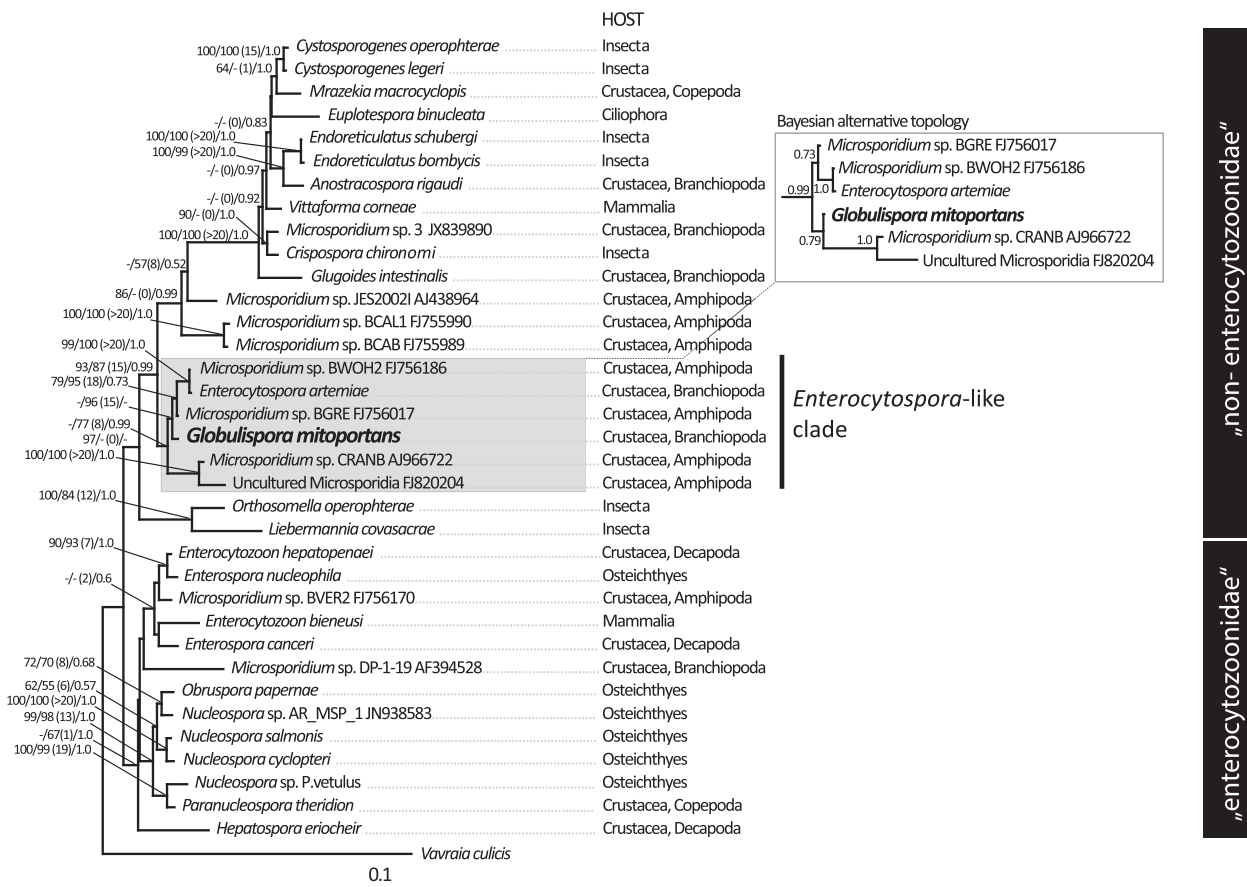


Fig. 28. Maximum likelihood tree based on microsporidian SSU rDNA sequences containing *Globulispora mitoportans*, n.g., n. sp. Numbers at the nodes represent the bootstrap values and the Bayesian posterior probability (ML/MP/BI) gaining more than 50% support (ML and MP) and 0.5 posterior probability (BI), respectively. Bremer indices are in the brackets following the MP bootstrap value. Scale bar is given under the tree. Microsporidian host group is indicated for each species. Bayesian tree topology of the Enterocytospora-like clade is in the white box. The “non-enterocytozoonidae” phylogenetic group contains various microsporidians of Crustacea and Insecta (with two exceptions). Its sister phylogenetic group “Enterocytozoonidae” contains microsporidians of Crustacea and Vertebrata in which polar filament precursors appear precociously in developmental stages.

otherwise, we presume that a single species, which we name *Globulispora mitoportans*, n.g., n. sp., infects both *D. pulex* and *S. vetulus*. We note that a very similar or even identical parasite exists in *Daphnia longispina* as documented in an unpublished electron micrograph made available to the authors of this paper by Dr. Dieter Ebert (Basel University, Switzerland) and Dr. R. Larsson (University of Lund, Sweden).

5.2. Structural characters

G. mitoportans has a unique structure among described and characterized microsporidia, consisting of three characters: thin spore walls, a globular polaroplast in spores and the presence of large mitosome-like vesicles with intravesicular material in both developmental stages and spores. Thin-walled spores typically occur in some primitive microsporidia, which are, however, distinct from *G. mitoportans* in host range and differ in a number of structural characters (lack of polaroplast membranes, reduced polar filament) (Larsson, 2014). Organization of the globular part of the polaroplast is unique among microsporidia; it does not correspond to any known polaroplast types reviewed by Vávra and Larsson (2014). The large double membrane vesicles (MLVs), occurring both in vegetative stages and in spores correspond structurally to mitosomes known in other microsporidia that are enveloped by a double membrane. They are, however much larger, contain intravesicular material, and also are present in mature

spores. The new information adds to the knowledge of the structural diversity of microsporidian mitosomes. Although considerable data characterizing the biochemistry of microsporidian mitosomes exists (Heinz and Lithgow, 2013), structural data is limited to four published papers in which mitosomes are respectively described as numerous, 50 × 90 nm vesicles with a double membrane and denser matrix present in vegetative stages of *Trachipleistophora hominis* (Williams et al., 2002); 50–200 nm double membrane vesicles present in vegetative stages, but also in spores of *Antonospora locustae* (Dolgikh et al., 2011); double membrane vesicles (150–200 × 100 nm) dispersed in the cytoplasm of vegetative stages and also accumulated in small groups near the spindle plaque of several microsporidia (Vávra, 2005). Vávra (2005) also observed larger (200–500 × 100–250 nm), lobed, double membrane vesicles with internal granules or membranous folds in the microsporidium *V. culicis*. The fourth report concerns the recently described microsporidium *Mitosporidium daphniae* in which a “mitochondrion-like structure with a double membrane” was seen in vegetative plasmodia (Haag et al., 2014). In contrast to these reports, the MLVs in *G. mitoportans* are very large (up to 1.5 μm) and division is synchronized with nuclear division. Our report also documents the occurrence of MLVs in mature spores in a form different from those in vegetative stages. Of interest is the internal matrix of material of moderate density, which is especially conspicuous in the MLVs contained in spores. This is the first clear evidence that some internal material inside microsporidian

Table 1
Microsporidian parasites of the gut epithelium of daphnids (Crustacea, Cladocera).

Organism	Authors	Spore size & shape (μm)	Polar tube coils	Polaroplast	Spore wall	Spore groups	Host
<i>Nosemooides simocephali</i>	Loubès and Akbarieh (1977)	2.5–3 × 1.5–1.75 oval	6–7	LP, VP	Ex-thin En-thick	SS	SV
<i>Baculea daphniae</i>	Loubès and Akbarieh (1978)	2.8–3 × 0.2 rod-like	No-coils	LP-reduced	Ex-thin En-medium	PV	DP
<i>Perezia diaphanosomaee</i>	Voronin (1988)	3.5–6.8 × 1.1–2.8 long oval to rod-like	4–6	LP (NL,WL)	Ex-thin En-thick	SS	DB
<i>Gluroides intestinalis</i>	Larsson et al. (1996)	2.4–2.7 × 1.1–1.7 ovoid, slightly kidney shaped	5–8 (6)	LP, 2 regions	Ex-medium En-thick	PV, SPOV	DM, DP
<i>Ordospora colligata</i>	Larsson et al. (1997)	2.32–3.69 × 1.33–2.29 pyriform	5–6	LP	Ex-thin En-thick	PV	DM
<i>Mitosporidium daphniae</i>	Haag et al. (2014)	2.31–2.67 × 1.05–1.29 ovoid or slightly bent	2	LP-concentric weakly developed	Ex-thin En-thick	SPOV	DM
<i>Globulispora mitoportans</i> gen. & sp. nov.	This paper	2.5 × 1.6 ovoid to oval	3–5	LP-reduced VP-reduced, GP-expanded	Ex-thin En-thin, atypical	SS	DP, SV

Abbreviations: En, endospore; Ex, exospore; DB, *Diaphanosoma brachyurum*; DM, *Daphnia magna*; DP, *Daphnia pulex*; GP, globular polaroplast; LP, lamellar polaroplast; NL, narrow lamellae; PW, parasitophorous vacuole; SPOV, sporophorous vesicle; SS, single spores; SV, *Simocephalus vetulus*; VP, vacuolar polaroplast; WL, wide lamellae.

mitosomes exists and its significance should be investigated. *G. mitoportans* is different from other microsporidia described to occur in the gut tissues of Cladocera. Six species of microsporidia, each belonging to a different genus were described from cladocera gut tissues: *Baculea daphniae* (Loubès and Akbarieh, 1978); *Gluroides intestinalis* (Larsson et al., 1996); *M. daphniae* (Haag et al., 2014); *Nosemooides simocephali* (Loubès and Akbarieh, 1977); *Ordospora colligata* (Larsson et al., 1997) and *Perezia diaphanosomaee* (Voronin, 1988). All these microsporidia are different from *Globulispora* in several respects (Table 1) and confirm the uniqueness of the new species and the proposed generic status.

5.3. Molecular phylogeny

The identity of sequences obtained from the three respective PCR products proved that a single strain of parasite existed in the host from which the DNA was obtained. Molecular phylogeny of *G. mitoportans* is unique in the sense that this microsporidian seems unrelated to all cladocera microsporidia for which molecular phylogeny data are presently available. The branch of the *Globulispora* containing clade is one of several branches representing a large clade containing a heterogenous assemblage of microsporidia infecting almost exclusively arthropods (insects and crustaceans) with two exceptions (one mammalian microsporidian and one microsporidian of a ciliophorean host), the “non-enterocytozoonidae clade” (Fig. 28). A single cladoceran microsporidian is represented at one of the branches of this clade, *G. intestinalis* infecting gut epithelium of *Daphnia magna* and *D. pulex*. *G. intestinalis* is phylogenetically distant from *G. mitoportans* and its fine structure is vastly different; it forms clusters of spores within a parasitophorous vacuole (Larsson et al., 1996). The “non-enterocytozoonidae clade” (Fig. 28) is a sister clade to microsporidia grouped in the “enterocytozoonidae clade”, assembling microsporidia infecting Crustacea and vertebrate hosts and structurally characterized by the precocious appearance of polar filament precursors in cytoplasm of developmental stages. Both clades contain microsporidia ranged to the superclade IV (“class Terresporidia”) of Vossbrinck and Debrunner-Vossbrinck (2005).

5.3.1. The Enterocytopspora-like clade

In microsporidia in general there is no strict congruity between structural and molecular phylogeny data. This led some authors to propose microsporidia as being “plastic parasites” (Stentiford et al., 2013). *Globulispora* in this respect is no exception. Its structure and development is different from its closest phylogeny counterpart *E. artemiae*, the only microsporidium in the clade for which structural data (although not very informative) are available. Development of *Enterocytopspora* takes place in parasitophorous vacuole, spores have different construction of the spore wall and their polaroplast seems to possess the typical lamellar and vacuolar parts (Rode et al., 2013). No structural data are available for the four microsporidia from amphipods in the *Globulispora* clade. Despite the discrepancy of structural data between *Globulispora* and *Enterocytopspora* cited above, the clade containing representatives of these two microsporidian genera, was stable in all performed phylogenetic analyses with relatively solid nodal support. Furthermore, topology tests strongly supported the stability of this clade. We feel therefore justified to propose the phylogeny clade *Enterocytopspora*-like.

6. Taxonomic summary

None of the so far known microsporidia genera have the combination of the characters discussed (Sections 5.2 and 5.3), which

raises the necessity to describe the present microsporidian as a representative of a new genus defined as below.

Phylum: Microsporidia (Balbiani, 1882).

Phylogeny clade: *Enterocytospora*-like.

Genus: *Globulispora* n. g.

6.1. Description

All life stages with isolated nuclei and in direct contact with host cell cytoplasm. Merogonial stages unknown. Division of ribbon-like sporogonial plasmodia by plasmotomy into unicellular fragments which transform into spores. Sporogonial stages have plasma membrane covered by a thin electrondense coat. Meiosis not observed. Spores ovoid to oval, with thin walls containing single nucleus and a tripartite polaroplast (several inconspicuous membranous lamellae, several larger vesicles and numerous electronlucent globules) in the anterior half of the spore. Posterior pole of the spore often drawn into a small protrusion representing posterior vacuole location. Polar filament isofilar.

6.2. Type species

Globulispora mitoportans, n. sp. Sporogonial stages have plasma membrane covered by 20 nm electrondense coat. Sporogonial stages contain large, electron lucent, double membrane vesicle, associated and dividing with the nucleus, and containing a loose web of material. Spores with character of the genus $2.5 \times 1.6 \mu\text{m}$ fresh, $2.5 \times 1.5 \mu\text{m}$ on dry, negatively stained smears, occurring singly, 30 nm endospore, 25–30 nm exospore of two layers covered by inconspicuous membrane, sometimes detached to form a sachet. Polaroplast with 5–8 membranous lamellae, several larger vesicles and numerous electronlucent globules among which one to several larger double membrane vesicles with dense central material, occur. Polar filament 3–5 coils, internal layering unresolved.

6.3. Etymology

alluding to the polaroplast globules in the spore and to the presence of conspicuous vesicles with double membrane believed to be mitosomes.

Type hosts, tissue and habitat midgut and gastric ceca epithelium of *Daphnia pulex* (Leydig, 1860). Additional host: *Simocephalus vetulus* (Müller, 1776). Forest marsh, near Běleč, Middle Bohemia region, Czech Republic ($50^{\circ}3'12.240''\text{N}$, $14^{\circ}1'4.221''\text{E}$).

6.4. Type material deposition

Slides with thick sections of resin block and with negatively stained spores are deposited in the International Protozoan Type Slide Collection, Department of Invertebrate Zoology, National Museum of Natural History, Smithsonian Institution, Washington, DC, USA, Account Nos. USNM (USNM Nos. 1283364, 1283365) and in respective slide collections of Jiří Vávra and Miroslav Hyliš at the Department of Parasitology and at Laboratory of Electron Microscopy, Faculty of Science, Charles University in Prague, Czech Republic. SSU rRNA gene sequence was deposited at GenBank Acc. No. KT762153.

Appendix A. Supplementary material

Supplementary data associated with this article can be found, in the online version, at <http://dx.doi.org/10.1016/j.jip.2016.02.003>.

References

- Andreadis, T.G., Takaoka, H., Otsuka, Y., Vossbrinck, C.R., 2013. Morphological and molecular characterization of a microsporidian parasite, *Takaokaspas nipponicus* n. gen., n. sp. from the invasive rock pool mosquito, *Ochlerotatus japonicus japonicus*. J. Invertebr. Pathol. 114, 161–172.
- Balbiani, G., 1882. Sur les microsporidies ou psorospermes des Articulés. C.R. Acad. Sci. Paris 95, 1168–1171.
- Becnel, J.J., 2012. Complementary techniques: preparations of entomopathogens and diseased specimens for more detailed study using microscopy. In: Lacey, L.A. (Ed.), Manual of Techniques in Invertebrate Pathology, second ed. Academic Press, pp. 451–466.
- Becnel, J.J., Andreadis, T.G., 2014. Microsporidia in insects. In: Weiss, L.M., Becnel, J.J. (Eds.), Microsporidia, Pathogens of Opportunity. Wiley Blackwell, pp. 521–570.
- Becnel, J.J., Takvorian, P.M., Cali, A., 2014. Checklist of available generic names for Microsporidia with type species and type hosts. In: Weiss, L.M., Becnel, J.J. (Eds.), Microsporidia, Pathogens of Opportunity. Wiley Blackwell, pp. 671–686.
- Dolgikh, V.V., Senderskiy, I.V., Pavlova, O.A., Naumov, A.M., Beznoussenko, G.V., 2011. Immunolocalization of an alternative respiratory chain in *Antonospora (Paranosema) locustae* spores: mitosomes retain their role in microsporidial energy metabolism. Eukaryot. Cell 10, 588–593.
- Galtier, N., Gouy, M., Gautier, C., 1996. SEAVIEW and PHYLO_WIN: two graphic tools for sequence alignment and molecular phylogeny. Comp. Appl. Biosci. 12, 543–548.
- Haag, K.L., James, T.Y., Pombert, J.-F., Larsson, R., Schaer, T.M.M., Refardt, D., Ebert, D., 2014. Evolution of a morphological novelty occurred before genome compaction in a lineage of extreme parasites. Proc. Natl. Acad. Sci. USA 111, 15480–15485.
- Heinz, E., Lithgow, T., 2013. Back to basics: a revealing secondary reduction of the mitochondrial protein import pathway in diverse intracellular parasites. Biochim. Biophys. Acta – Mol. Cell Res. 1833, 295–303.
- James, T.Y., Pelin, A., Bonen, L., Ahrendt, S., Sain, D., Corradi, N., Stajich, J.E., 2013. Shared signatures of parasitism and phylogenomics unite cryptomycota and microsporidia. Curr. Biol. 23, 1548–1553.
- Karpov, S.A., Mamkaeva, M.A., Aleoshin, V.V., Nessonova, E., Lilje, O., Gleason, F.H., 2014. Morphology, phylogeny, and ecology of the aphelids (Aphelidea, Opisthokonta) and proposal for the new superphylum Opisthosporidia. Front. Microbiol. 5, 112.
- Katoh, K., Kuma, K., Toh, H., Miyata, T., 2005. MAFFT version 5: improvement in accuracy of multiple sequence alignment. Nucl. Acids Res. 33, 511–518. <http://dx.doi.org/10.1093/nar/gki198>.
- Keeling, P.J., 2014. Phylogenetic place of Microsporidia in the tree of Eukaryotes. In: Weiss, L.M., Becnel, J.J. (Eds.), Microsporidia, Pathogens of Opportunity. Wiley Blackwell, pp. 195–202.
- Larsson, J.I.R., 2014. The primitive Microsporidia. In: Weiss, L.M., Becnel, J.J. (Eds.), Microsporidia, Pathogens of Opportunity. Wiley Blackwell, pp. 605–634.
- Larsson, J.I.R., Ebert, D., Vávra, J., Voronin, V.N., 1996. Redescription of *Pleistophora intestinalis* Chatton, 1907, a microsporidian parasite of *Daphnia magna* and *Daphnia pulex*, with establishment of the new genus *Glugoides* (Microspora, Glugeidae). Eur. J. Protistol. 32, 251–261.
- Larsson, J.I.R., Ebert, D., Vávra, J., 1997. Ultrastructural study and description of *Ordoospora colligata* gen. et sp. nov. (Microspora, Ordoспориды fam. nov.), a new microsporidian parasite of *Daphnia magna* (Crustacea, Cladocera). Eur. J. Protistol. 33, 432–443.
- Leydig, F., 1860. Naturgeschichte der Daphniden (Crustacea Cladocera). Laupp & Siebeck, Tübingen, p. 252.
- Loubès, C., Akbarieh, M., 1977. Étude ultrastructurale de *Nosemoides simocephali* n. sp. (Microsporidie), parasite intestinal de la Daphnie *Simocephalus vetulus* Müller, 1776. Z. Parasitenkd. 54, 125–137.
- Loubès, C., Akbarieh, M., 1978. Étude ultrastructurale de la microsporidie *Baculea daphniae* n.g., n.sp., parasite de l'épithélium intestinal de *Daphnia pulex* Leydig, 1860 (Crustacé, Cladocère). Protistologica 14, 23–38.
- Müller, O.F., 1776. Zoologiae Danicae prodromus, seu animalium Daniae et Norvegiae indigenarum characteres, nomina et synonyma imprimis popularium. Typis Hallageris, Havniae, p. 282.
- Rambaut, A., Drummond, A.J., 2007. Tracer v1.4 <<http://beast.bio.ed.ac.uk/Tracer>>.
- Refardt, D., Decaestecker, E., Johnson, P.T.J., Vávra, J., 2008. Morphology, molecular phylogeny, and ecology of *Binucleata daphniae* n. g., n. sp. (Fungi: Microsporidia), a parasite of *Daphnia magna* Straus, 1820 (Crustacea: Branchiopoda). J. Eukaryot. Microbiol. 55, 393–408.
- Rode, N.O., Landes, J., Lievens, E.J.P., Flaven, E., Segard, A., Jabbour-Zahab, R., Michalakis, Y., Agnew, P., Vivares, C.P., Lenormand, T., 2013. Cytological, molecular and life cycle characterization of *Anostracospora rigaudi* n. g., n. sp. and *Enterocytospora artemiae* n. g., n. sp., two new microsporidian parasites infecting gut tissues of the brine shrimp *Artemia*. Parasitology 140, 1168–1185.
- Ronquist, F., Huelsenbeck, J.P., 2003. MrBayes 3: Bayesian phylogenetic inference under mixed models. Bioinformatics 19, 1572–1574. <http://dx.doi.org/10.1093/bioinformatics/btg180>.
- Shimodaira, H., Hasegawa, M., 2001. CONSEL: for assessing the confidence of phylogenetic tree selection. Bioinformatics 17, 1246–1247. <http://dx.doi.org/10.1093/bioinformatics/17.12.1246>.
- Slothouber Galbreath, J.G.M., Smith, J.E., Becnel, J.J., Butlin, R.K., Dunn, A.M., 2010. Reduction in post-invasion genetic diversity in *Crangonyx pseudogracilis* (Amphipoda: Crustacea): a genetic bottleneck or the work of hitchhiking vertically transmitted microparasites? Biol. Invas. 12, 191–209.

- Snowden, K.F., 2014. Microsporidia in higher vertebrates. In: Weiss, L.M., Becnel, J.J. (Eds.), *Microsporidia, Pathogens of Opportunity*. Wiley Blackwell, pp. 469–492.
- Stamatakis, A., 2006. RAxML-VI-HPC: maximum likelihood-based phylogenetic analyses with thousands of taxa and mixed models. *Bioinformatics* 22, 2688–2690. <http://dx.doi.org/10.1093/bioinformatics/btl446>.
- Stentiford, G.D., Dunn, A.M., 2014. Microsporidia in aquatic invertebrates. In: Weiss, L.M., Becnel, J.J. (Eds.), *Microsporidia, Pathogens of Opportunity*. Wiley Blackwell, pp. 579–604.
- Stentiford, G.D., Bateman, K.S., Feist, S.W., Chambers, E., Stone, D.M., 2013. Plastic parasites: extreme dimorphism creates a taxonomic conundrum in the phylum Microsporidia. *Int. J. Parasitol.* 43, 339–352.
- Stöver, B.C., Müller, K.F., 2010. TreeGraph 2: combining and visualizing evidence from different phylogenetic analyses. *BMC Bioinf.* 11, 9. <http://dx.doi.org/10.1186/1471-2105-11-7>.
- Swofford, D.L., Waddell, P.J., Huelsenbeck, J.P., Foster, P.G., Lewis, P.O., Rogers, J.S., 2001. Bias in phylogenetic estimation and its relevance to the choice between parsimony and likelihood methods. *System. Biol.* 50, 525–539. <http://dx.doi.org/10.1080/106351501750435086>.
- Vávra, J., 2005. “Polar vesicles” of microsporidia are mitochondrial remnants (“mitosomes”)? *Folia Parasitol.* 52, 193–195.
- Vávra, J., Larsson, J.I.R., 2014. Structure of Microsporidia. In: Weiss, L.M., Becnel, J.J. (Eds.), *Microsporidia, Pathogens of Opportunity*. Wiley Blackwell, pp. 1–70.
- Vávra, J., Lukeš, J., 2013. Microsporidia and ‘The Art of Living Together’. In: Rollinson, D. (Ed.), *Advances in Parasitology*, vol. 82. Academic Press, pp. 253–320.
- Vávra, J., Maddox, J.V., 1976. Methods in microsporidiology. In: Bulla, L.A., Jr., Cheng, T.C. (Eds.), *Comparative Pathobiology*, vol. 1. Plenum Press, New York, pp. 281–319.
- Voronin, V.N., 1988. The ultrastructure of the microsporidian *Perezia diaphanosomae* (Voronin, 1977). *Citologiya* 30, 770–773 (in Russian).
- Vossbrinck, V.R., Debrunner-Vossbrinck, B.A., 2005. Molecular phylogeny of the Microsporidia: ecological, ultrastructural and taxonomic considerations. *Folia Parasitol.* 52, 131–142.
- Weiss, L.M., Vossbrinck, C.R., 1999. Molecular biology, molecular phylogeny, and molecular diagnostic approaches to the microsporidia. In: Wittner, M., Weiss, L. M. (Eds.), *The Microsporidia and Microsporidiosis*. AMS Press, Washington, DC, pp. 129–171.
- Williams, B.A.P., Hirt, R.P., Lucocq, J.M., Embley, T.M., 2002. A mitochondrial remnant in the microsporidian *Trachipleistophora hominis*. *Nature* 418, 865–869.